

# Spatiotemporal Response of Maize Yield to Edaphic and Meteorological Conditions in a Saline Farmland

Elia Scudiero,\* Pietro Teatini, Dennis L. Corwin, Nicola Dal Ferro, Gianluca Simonetti, and Francesco Morari

## ABSTRACT

Spatiotemporal variability of crop production strongly depends on soil heterogeneity, meteorological conditions, and their interaction. Canopy reflectance can be used to describe crop status and yield spatial variability. The objectives of this work were to understand the spatiotemporal variability of maize (*Zea mays* L.) yield using ground-based reflectance acquisitions in a salinity- and water-stress-affected 21-ha field beside the Venice Lagoon, Italy. Intra- and interannual reflectance variations were analyzed across the entire field and at each map cell with time to understand how the different soil-related stresses (i.e., salinity and water) arise under different meteorological conditions. The results show that the normalized difference vegetation index (NDVI) acquired during the maize flowering and kernel maturation stages (during the three growing seasons of 2010, 2011, and 2012) effectively described yield spatiotemporal variability. In particular, stressed areas exhibited the smallest changes in NDVI during a single growing season. Soil salinity and water stress were responsible for approximately 44% of the intra-annual NDVI change. When multiyear NDVI data are compared, areas affected by soil salinity show the smallest temporal variability. Nevertheless, areas that are slightly saline and constantly affected by water stress could not be distinguished from highly saline areas. Multiyear reflectance data can be a useful tool to characterize areas where soil salinity is the main factor limiting crop production. In areas where several plant stresses occur simultaneously every year, the proposed approach could be used to guide precision irrigation to make adjustments for within-field leaching requirement and/or irrigation needs.

**Yield maps provide pivotal information** to implement precision agriculture techniques. The delineation of input prescription maps (e.g., map of site-specific management units, fertilizer, irrigation water, etc.) relies on a careful study of input prescription maps and their interaction with edaphic (i.e., soil-related) properties. When focusing on production variability at the field or farm scale, yield maps from multiple years should be considered (Blackmore, 2000; Blackmore et al., 2003) because approximately half of the variation in each map generally comes from year-to-year variation (McBratney et al., 2005).

Most crop yield studies, however, focus only on describing the spatial variability of productivity despite the potential benefit of considering the effects of the spatial and temporal variability of the plant–soil relationship (McBratney et al., 2005). Indeed, soil–plant interactions are believed to be the largest contributors to yield spatial variability (Corwin et al., 2003; Scudiero et al.,

2013). These interactions, however, are influenced by seasonal factors, such as meteorological conditions (e.g., rainfall) and anthropogenic activities (e.g., irrigation).

Similar to many delta plains around the world, the southern margin of the Venice Lagoon, Italy, is an area characterized by contrasting soils and saltwater intrusion (de Franco et al., 2009; Scudiero et al., 2012, 2013). Soil salinity and water stress considerably limit crop yield in the area (Manoli et al., 2013; Scudiero et al., 2013). These two plant stresses are generally difficult to distinguish from one another (Elmetwalli et al., 2012; Hu et al., 2007; Munns, 2002) because they both decrease the soil water potential, normally leading to similar physiological responses (Munns, 2002). Nevertheless, especially in regions where salinity is the major cause of crop loss, its effects on yield are generally more stable with time because salinity is often less dependent on annual variability in precipitation (Lobell et al., 2007, 2010; Madrigal et al., 2003). On the other hand, water stress is generally more dependent on meteorological conditions (and irrigation), especially in areas characterized by low water retention.

To better understand plant growth and yield response, crop canopy reflectance is often studied (Mulla, 2013). Reflectance is used to estimate crop stress status (Blackmer et al., 1995; Vina et al., 2004) and predict production (Shanahan et al., 2001). Reflectance ground-based and satellite sensors can be

E. Scudiero, and D.L. Corwin, USDA–ARS, U.S. Salinity Lab., 450 West Big Springs Rd., Riverside, CA 92507-4617; E. Scudiero, N. Dal Ferro, G. Simonetti, and F. Morari, Dep. of Agronomy, Food, Natural Resources, Animals, and Environment (DAFNAE), Univ. of Padua, Viale dell'Università 16, Legnaro 35020, Italy; and P. Teatini, Dep. of Civil, Environmental, and Architectural Engineering (ICEA), Univ. of Padua, Via Trieste 63, Padua 35121, Italy. Received 24 Feb. 2014. \*Corresponding author (scudiero@dmsa.unipd.it).

Published in *Agron. J.* 106:2163–2174 (2014)  
doi:10.2134/agronj14.0102

Copyright © 2014 by the American Society of Agronomy, 5585 Guilford Road, Madison, WI 53711. All rights reserved. No part of this periodical may be reproduced or transmitted in any form or by any means, electronic or mechanical, including photocopying, recording, or any information storage and retrieval system, without permission in writing from the publisher.

**Abbreviation:** DGPS, differential global positioning system; NDVI, normalized difference vegetation index; NDVI\_SpT, spatial trend of normalized difference vegetation index; SDVI, temporal variability of normalized difference vegetation index; SSMU, site-specific management unit.

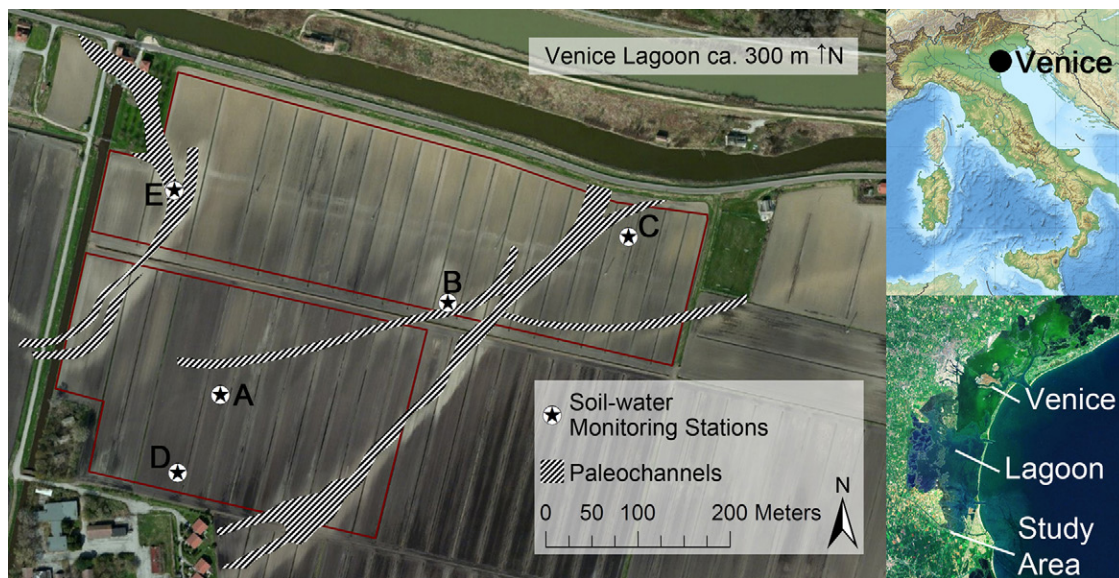


Fig. 1. Map of the study area depicting the five soil-water monitoring stations (A, B, C, D, and E) and the paleochannels.

used to monitor canopy development with a very high spatial resolution ( $<4 \text{ m}^2$ ) (Mulla, 2013; Solari et al., 2008), providing more accurate information than yield maps. Yield maps are normally characterized by coarser resolution and noise in the data due to yield monitor and combine dynamics (Blackmore, 1999; Corwin et al., 2003; Ping and Dobermann, 2005). In fact, high-resolution maps of canopy reflectance can be used as an ancillary variable to increase the accuracy of yield maps (Dobermann and Ping, 2004). In addition to multiseasonal (i.e., interannual) information, canopy reflectance can also be used to monitor spatiotemporal within-season (i.e., intra-annual) variations, providing useful information for decision making in agriculture practices.

The general goal of this study was to identify a method based on remote sensing to help delineate input prescription maps in saline fields. The specific objective was to understand the spatiotemporal variability of maize yield using ground-based reflectance acquisitions on a salinity-affected field at the southern margin of the Venice Lagoon, Italy. To do so, the relationships between yield and canopy reflectance maps were initially studied for ground-truthing purposes. Subsequently, the intra- and interannual spatial and temporal variability of maize reflectance were analyzed to understand how the different soil-related stress types arise under different meteorological conditions. The major challenge of this work was to distinguish the effects of water stress from salinity stress on maize production using observations describing the soil spatial variability, meteorological data, and their interactions.

## MATERIALS AND METHODS

### The Study Area

The study was performed on a 21-ha field affected by soil salinity located in Chioggia, Italy ( $45^{\circ}10'57'' \text{ N}$ ,  $12^{\circ}13'55'' \text{ E}$ ), along the southern margin of the Venice Lagoon (Fig. 1). The site lies below mean sea level, from  $-1$  to  $-3.3$  m, and was reclaimed for agriculture purposes at the beginning of the 20th century. A pumping station and a dense network of open ditches control the depth of the water table, which is maintained fairly shallow

in summer to promote subirrigation. The water table ranges from  $-0.5$  to  $-1.8$  m below ground level, with little vertical variation ( $\sim 5$  cm) during the year. Only a very limited portion ( $<5\%$ ) of the field is characterized by a very shallow water table ( $<0.7$  m) (Manoli et al., 2014). The soil is predominantly a silty clay (Molli-Gleyic Cambisol, FAO-UNESCO, 1989), with the presence of acidic peat and sandy drifts (i.e., paleochannels) crossing the study site in a southwest to northeast direction. A detailed description of the soil variability can be found in Scudiero et al. (2013).

Scudiero et al. (2013) identified soil salinity, texture, bulk density, and soil organic C as major factors affecting maize productivity and accordingly delineated five site-specific management units (SSMUs) within the experimental site (Fig. 2; Table 1). More precisely, the classification identified a peaty, acidic, moderately saline, and sandy area (SSMU I); a very saline zone (SSMU II); a nonsaline area comprising the coarser portions of the paleochannels (SSMU III); a zone with the best conditions for maize growth (SSMU IV) characterized by mid to low salinity, mid to low peaty content, and the highest clay content; and a peaty, acidic, moderately saline, and silty unit (SSMU V). The variability of soil salinity, texture, bulk density, and organic C within each management unit is shown in Fig. 2b.

To assess saline and water stress, five monitoring stations were placed at the study site (Table 1). Each station was equipped with capacitance-resistance probes (ECH2O-5TE, Decagon Devices), to measure the water content and pore-water salinity (Scudiero et al., 2012), and tensiometers (T4e, UMS GmbH) to record the soil-water potential at depths of 10, 30, 50, and 70 cm. The sensors were connected to a datalogger and data were recorded hourly. The water table level at each station was monitored every second week using phreatic wells. The five monitoring stations, described in Table 1, were named A, B, C, D, and E (Fig. 1). Unfortunately, since the zonal definition was performed later than the station installation, SSMU IV was not monitored by any of the stations, whereas two stations (B and E) were located in SSMU III.

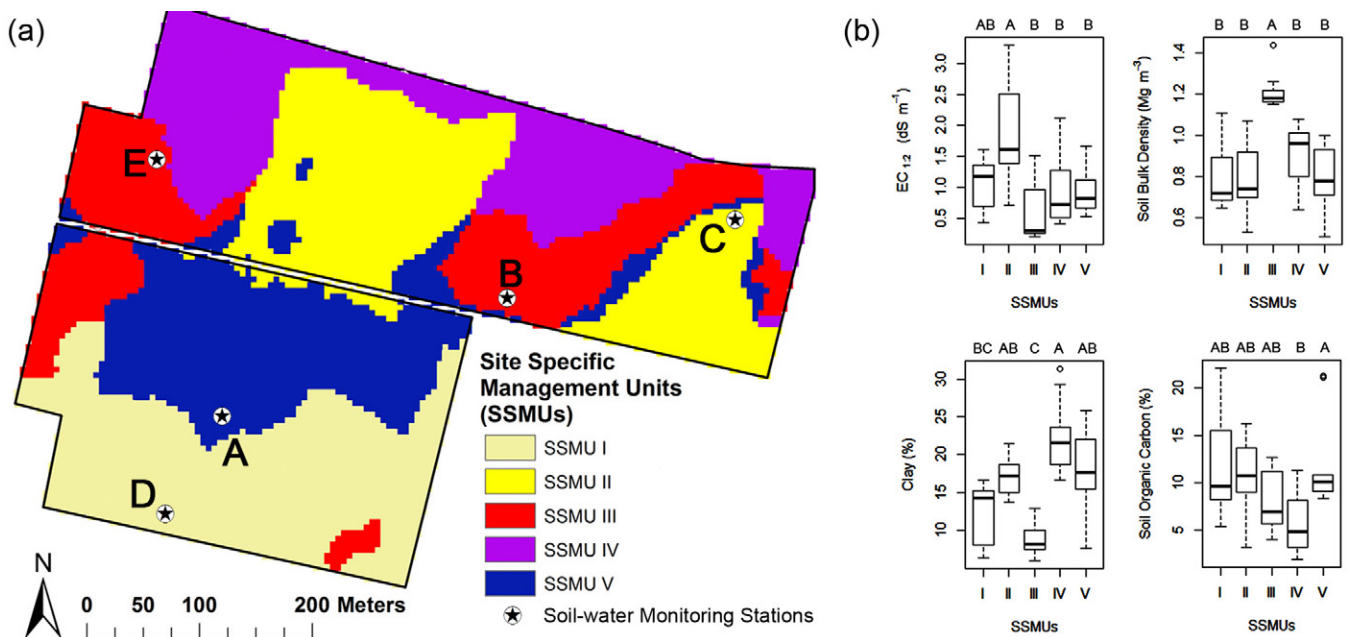


Fig. 2. The (a) five management zones and (b) boxplots for, electrical conductivity of a soil extract with a soil to water ratio of 1:2 ( $EC_{1,2}$ ), soil bulk density, soil organic C content, and clay content. The bold lines crossing the rectangles represent the median values; circles represent outliers. Within plots, boxes topped with the same uppercase letter are not significantly different ( $P < 0.05$ ) as presented by Scudiero et al. (2013).

### Maize Cultivation and Yield Monitoring

Rainfed maize was cultivated in 2010 (seeding 22 April and harvest 10 September), 2011 (seeding 4 April 4 and harvest 2 September), and 2012 (seeding 21 March and harvest 11 September). Soil tillage was an autumn plowing to the 30-cm depth, followed by standard seedbed preparation operations. Maize was fertilized with a base dressing of 64 kg N ha<sup>-1</sup> and 94 kg P<sub>2</sub>O<sub>5</sub> ha<sup>-1</sup> and a topdressing of 184 kg N ha<sup>-1</sup> (urea).

Maize yield was measured by a combine harvester equipped with a yield monitor (Agrocom, Claas) and a differential global positioning system (DGPS). Data were recorded by the yield monitor at a density of 1 measure per approximately 70 m<sup>2</sup>. Data sets were standardized across a 10- by 10-m grid (i.e., 1906 cells) using a 10-m search radius and the procedures of Blackmore (1999) and Blackmore et al. (2003) because coarser resolutions would not accurately represent yield patterns. In 2012, limited portions of the sandy paleochannels were characterized by a lack of grain productivity. Therefore, a 0 Mg ha<sup>-1</sup> yield value was manually assigned to the cells corresponding to such zones.

### Ground-Based Reflectance Acquisitions

Maize reflectance at 590 ± 5.5 nm (visible or VIS) and at 880 ± 5.5 nm (near infrared or NIR) was measured with an active spectrometer (ACS-210 CropCircle, Holland Scientific) linked with a GPS. Reflectance was acquired three times a year as follows: on 9 and 23 July and 16 Aug. 2010; on 4 and 14 July and 5 Aug. 2011; and on 15 and 27 June and 19 July 2012. The site was covered each time with approximately 6000 acquisition points, using a 5-s time acquisition interval. The CropCircle (CC) was held on a pole at approximately 0.8 m above the maize canopy, assessing reflectance over an ~0.1- by 0.5-m area (Solari et al., 2008), perpendicular to the maize row direction. The readings of the CC sensor penetrate up to six leaf levels in the maize canopy (Solari, 2006). The CC data were used to calculate the well-known normalized difference vegetation index (NDVI) (Rouse et al., 1974):

$$NDVI = \frac{NIR - VIS}{VIS + NIR} \quad [1]$$

Table 1. Soil electrical conductivity ( $EC_e$ ), texture, bulk density ( $\rho_b$ ), soil organic C (SOC), and volumetric water content at field capacity (FC) and the wilting point (WP) in the root zone (data for the 0–60-cm soil profile) at the five soil-water monitoring stations in the soil-specific management units (SSMUs). Soil samples from 2010 (Scudiero et al., 2013).

Monitoring station	$EC_e$	Sand	Silt	Clay	$\rho_b$	SOC	FC	WP
	dS m <sup>-1</sup>							
A (SSMU V)	1.90	31.06	47.17	21.77	0.95	10.61	0.48	0.30
B (SSMU III)	0.33	68.46	24.33	7.21	1.12	4.48	0.36	0.25
C† (SSMU II)	5.45	36.87	44.76	18.37	0.69	11.78	0.51	0.31
D (SSMU I)	2.94	41.98	42.38	15.64	0.73	21.02	0.43	0.29
E (SSMU III)	0.02	71.12	19.86	9.01	1.44	12.57	0.20	0.09

† Data for the 0–40 cm soil profile because the water table was shallower than 70 cm at this location.

## Normalized Difference Vegetation Index and Yield Spatial and Temporal Variability

The spatial correlation structure of each NDVI data set ( $\delta_i$ ) was described with an isotropic exponential semivariogram  $v$ :

$$v(\delta_i) = (\eta + \sigma^2) \left[ 1 - \exp\left(-\frac{h}{r}\right) \right] \quad [2]$$

where  $\eta$  represents the nugget variance,  $\sigma^2$  the spatial variance component (partial sill),  $h$  the lag distance, and  $r$  the range. Because the NDVI distribution was not normal, the data sets were preliminarily normalized by Box–Cox transformation (Box and Cox, 1964). Maps of the NDVI were produced using ordinary kriging and their goodness of fit was tested with a leave-one-out cross-validation procedure using ArcMap 10.1 (ESRI). Finally, the maps were gridded with 10- by 10-m cells to match the yield maps.

Spatial and temporal variances of the yield data sets were determined according to Whelan and McBratney (2000) for the entire field and for each SSMU. The spatial variance  $\sigma_s^2$  was calculated by averaging the maize production during the 3 yr and calculating the variance of the average data set:

$$\sigma_s^2 = \frac{1}{N_c - 1} \times \sum_{j=1}^{N_c} \left[ \frac{1}{N_y} \sum_{i=1}^{N_y} Y_{i,j} - \frac{1}{N_c} \sum_{j=1}^{N_c} \left( \frac{1}{N_y} \sum_{i=1}^{N_y} Y_{i,j} \right) \right]^2 \quad [3]$$

where  $N_y$  and  $N_c$  are the number of available yield maps and the cells of each map, respectively, and  $Y_{i,j}$  is the yield at the  $i$ th year in the  $j$ th cell. The temporal variance  $\sigma_t^2$  was calculated by averaging the yield variance across the 3 yr at each cell of the 10- by 10-m grid:

$$\sigma_t^2 = \frac{1}{N_c} \sum_{j=1}^{N_c} \left[ \frac{1}{N_y - 1} \sum_{i=1}^{N_y} \left( Y_{i,j} - \frac{1}{N_y} \sum_{i=1}^{N_y} Y_{i,j} \right)^2 \right] \quad [4]$$

Spatial ( $\sigma_s^2$ ) and temporal ( $\sigma_t^2$ ) variances help to quantify the yield variability across the area during the 3 yr but do not help to understand the spatial structure of the data and the changes with time of such spatial structures.

When spatial data sets of crop yield and NDVI at different times are available, maps of spatial trend and temporal variability can be produced (Blackmore, 2000). Yield spatial trend (Y\_SpT) maps were obtained as the average yield at each cell during the 3 yr. Maps of the NDVI spatial trend (NDVI\_SpT) were developed for each year to analyze the intra-annual spatial trend (i.e., averaging the maps from the three surveys performed each year) and during the 3 yr using all nine surveys for an interannual analysis.

Maps of temporal variability were produced as proposed by Tweed et al. (2007). Temporal variability of the NDVI at each  $j$ th cell of the grid is represented by its standard deviation (SDVI) with time:

$$SDVI_j = \sqrt{\frac{1}{N_{\text{surv}} - 1} \sum_{i=1}^{N_{\text{surv}}} (NDVI_i - NDVI_{\text{mean}})^2} \quad [5]$$

where  $N_{\text{surv}}$  is the number of processed surveys and  $NDVI_{\text{mean}}$  is the average NDVI for each cell across  $N_{\text{surv}}$ . Maps of SDVI were developed for both intra-annual ( $N_{\text{surv}} = 3$ ) and interannual ( $N_{\text{surv}} = 9$ ) temporal variability. The temporal standard deviation of yield ( $Y\_SD$ ) was also derived according to Eq. [5] as proposed by Blackmore (2000).

## Statistical Analyses

The maize production and NDVI maps were analyzed for both Pearson and spatial correlations. The spatial relations between maps were investigated using the experimental cross-covariance function (Goovaerts, 1997). When spatial correlation between two studied variables is sizeable, the cross-covariogram is characterized by non-null values for short lags and approaches zero increasing the number of lags. The spatial correlation can be either positive or negative. The larger the cross-covariance at short lags and the larger the distance at which the cross-covariogram tends to zero, the stronger the spatial correlation between the studied variables. The experimental cross-covariance functions were calculated with ArcMap 10.1 and fitted with exponential models.

Differences in yield and NDVI values, their spatial patterns, and the temporal variability within each SSMU were tested using the nonparametric Kruskal–Wallis rank test (Kruskal and Wallis, 1952). This test was selected instead of the classical analysis of variance because assumptions of the latter were not met by the available data sets (Acevedo-Opazo et al., 2008).

## Effects of Water and Salinity Stress on Normalized Difference Vegetation Index Temporal Variability

Intra-annual NDVI variability at the five soil-water monitoring stations was studied to understand the effects of soil salinity, texture, bulk density, and meteorological conditions.

Salinity and water stress may result in reduced plant growth and subsequently in lower evapotranspiration (Allen et al., 1998; Munns, 2002). The soil salinity and water stress effects on crop evapotranspiration are generally additive (Allen et al., 1998; Letey and Dinar, 1986). The decrease in crop evapotranspiration at different water and soil salinity stress levels during the growing season can be summarized using the evapotranspiration reduction coefficient  $K_s$  (Allen et al., 1998). When crop evapotranspiration is not affected by water scarcity and soil salinity,  $K_s = 1$ . Otherwise  $K_s$  decreases, with  $K_s = 0$  when plant transpiration ceases and only soil evaporation takes place (Allen et al., 1998). The  $K_s$  can be quantified as (Allen et al., 1998)

$$K_s = \left[ 1 - \frac{b}{K_y 100} (EC_e - EC_{e,\text{threshold}}) \right] \times \frac{TAW - D_r}{(1 - p^*) TAW} \quad [6]$$

where  $K_y$  is a coefficient describing the relative yield loss due to the reduction in crop actual evapotranspiration compared with

the potential evapotranspiration under standard conditions ( $ET_c$ ,  $\text{mm d}^{-1}$ ) caused by soil water shortage and set at 1.25 for maize (Allen et al., 1998);  $EC_e$  ( $\text{dS m}^{-1}$ ) is the soil salinity measured according to Rhoades et al. (1999);  $EC_{e\_threshold}$  ( $\text{dS m}^{-1}$ ) is the threshold below which productivity is not affected by soil salinity, equal to  $1.7 \text{ dS m}^{-1}$  in maize (Maas, 1996);  $b$  is the yield reduction percentage per unit increase in soil salinity ( $\text{dS m}^{-1}$ ) when  $EC_e > EC_{e\_threshold}$ , set to 12 for maize (Maas, 1996);  $D_r$  (mm) is the difference between the volumetric water content measured in the root zone and the volumetric water content at field capacity, TAW (mm) is the root-zone total available soil water (i.e., the difference between the volumetric water content at field capacity and at the wilting point), and  $p^*$  is the fraction (varies according to crop type and  $ET_c$ ) of TAW that plants can extract from the root zone without suffering water stress ( $0.1 \leq p^* \leq 0.8$ ). According to Eq. [6], salinity  $> EC_{e\_threshold}$  reduces  $K_s$  even if water stress does not occur.

Equation [6] was computed on a daily time frame using the hydrologic records at the monitoring stations. The daily  $K_s$  variations at the monitoring stations were compared with the intra-annual variations in the NDVI. To do so, the NDVI variations between consecutive surveys were expressed as average daily NDVI change ( $\Delta\text{NDVI}$ ).

The volumetric water content ( $\theta$ ,  $\text{m}^3 \text{ m}^{-3}$ ) was estimated at each monitoring station from the measured soil dielectric constant and apparent electrical conductivity using the equation proposed by Scudiero et al. (2012):

$$\theta = (a' + a''EC_a)[1 + q \ln(\epsilon_r)] \quad [7]$$

where  $EC_a$  is the apparent (i.e., bulk) soil electrical conductivity ( $\text{dS m}^{-1}$ ),  $\epsilon_r$  (dimensionless) is the soil dielectric complex permittivity, and  $q$ ,  $a'$ , and  $a''$  are fitting parameters that, for the Chioggia soils, are  $-0.766$ ,  $-0.352 - 0.006 \times \text{soil organic C (\%)}$ , and  $0.020 - 0.009 \times [\text{clay (\%)/sand (\%)}]$ , respectively. Water content in the root zone was calculated by averaging the data from the upper three probes (i.e., 10, 30, and 50 cm deep). Indeed, despite the fact that maize roots can grow deeper than 1 m, most of the root system is normally found in the top 0.5 m (Sharp and Davies, 1985). The stations were operative from 28 July 2010, 15 May 2011, and 26 April 2012 to a few days after maize harvesting. In 2010, Stations D and E were unavailable. Water contents at field capacity and the wilting point were measured by means of a pressure plate apparatus at  $-33 \text{ kPa}$  and

$-1.5 \text{ MPa}$ , respectively, on undisturbed soil samples taken at each station at the 10-, 30-, and 50-cm depths (Table 1).

The meteorological data recorded by a nearby automatic station (Regional Agency for Environmental Protection, Veneto) were used to calculate  $ET_c$  using the Penman–Monteith equation with the dual-crop coefficient approach (Allen et al., 1998). Temperature records were also used to calculate the growing degree days (GDD), setting the base temperature equal to  $8^\circ\text{C}$ . Note that, for the maize used at the study site, the emergence (VE), seven-leaf (V7), early tassel (R1), kernel blister (R2), beginning dent (R4), and maturity (R6) growth stages started at 60, 200, 760, 960, 1355, and 1620 cumulative GDD, respectively, after sowing. Surveys of NDVI (i, ii, and iii) were performed in 2010 during early tassel (R1, at 853 GDD), kernel blister (R2, at 1097 GDD), and early beginning dent (R4, at 1409 GDD), respectively. In 2011, Surveys i, ii, and iii were performed during R1 (at 889 GDD), R2 (at 1051 GDD), and right before the start of R4 (at 1342 GDD), respectively. In 2012, NDVI was acquired right before the start of R1 (at 597 GDD), during R1 (at 789 GDD), and during R2 (at 1149 GDD), respectively. All the surveys were performed in the reproduction phase when the basal crop coefficient describing maize transpiration throughout the growing season (Allen et al., 1998) was at maximum (i.e., “mid-season”).

## RESULTS AND DISCUSSION

### Meteorological Data

Precipitation differed substantially during the three growing seasons (Table 2) and was also quite unusual with respect to the average April to September rainfall from 1993 to 2012, which amounts to 360 mm. Indeed, the 2010 growing season was fairly rainy (i.e., in the upper third quartile, 534.6 mm), whereas the following two growing seasons were rather dry (i.e., both in the first quartile, 199.8 mm in 2011, 150.6 mm in 2012). Rainfall in 2010 and 2011 was evenly spread throughout the season. Contrarily, the low 2012 precipitation occurred almost exclusively during the maize vegetative phase. No precipitation occurred during the early tassel (R1) and kernel blister (R2) reproductive stages, which are known to be among the most critical stages of maize growth (Abendroth et al., 2011; NeSmith and Ritchie, 1992). The daily average reference evapotranspiration ( $ET_0$ ) was 4.01, 4.42, and  $4.08 \text{ mm d}^{-1}$ , whereas the  $ET_0$  across the entire season was 569, 672, and 717 mm in 2010, 2011, and 2012, respectively.

Table 2. Date and total rainfall during the maize growing season in 2010, 2011, and 2012 at sowing, harvesting, beginning of relevant physiological stages, and normalized difference vegetation index survey days.

Maize growth stage†	2010		2011		2012	
	Date	Cumulative rainfall mm	Date	Cumulative rainfall mm	Date	Cumulative rainfall mm
Sowing	22 Apr.	0.0	4 Apr.	2.4	21 Mar.	0.0
VE	29 Apr.	5.2	13 Apr.	8.6	4 Apr.	1.2
V7	19 May	129.8	8 May	18.0	5 May	54.6
R1	4 July	292.6	25 June	136.6	26 June	134.8
R2	15 July	292.8	10 July	148.0	7 July	134.8
R4	12 Aug.	410.0	6 Aug.	191.0	2 Aug.	141.0
R6	1 Sept.	534.6	24 Aug.	199.8	19 Aug.	150.6
Harvest	10 Sept.	539.0	2 Sept.	200.0	11 Sept.	251.4

† VE, beginning of emergence; V7, seven-leaf; R1, early tassel; R2, kernel blister; R4, beginning dent; R6, maturity.

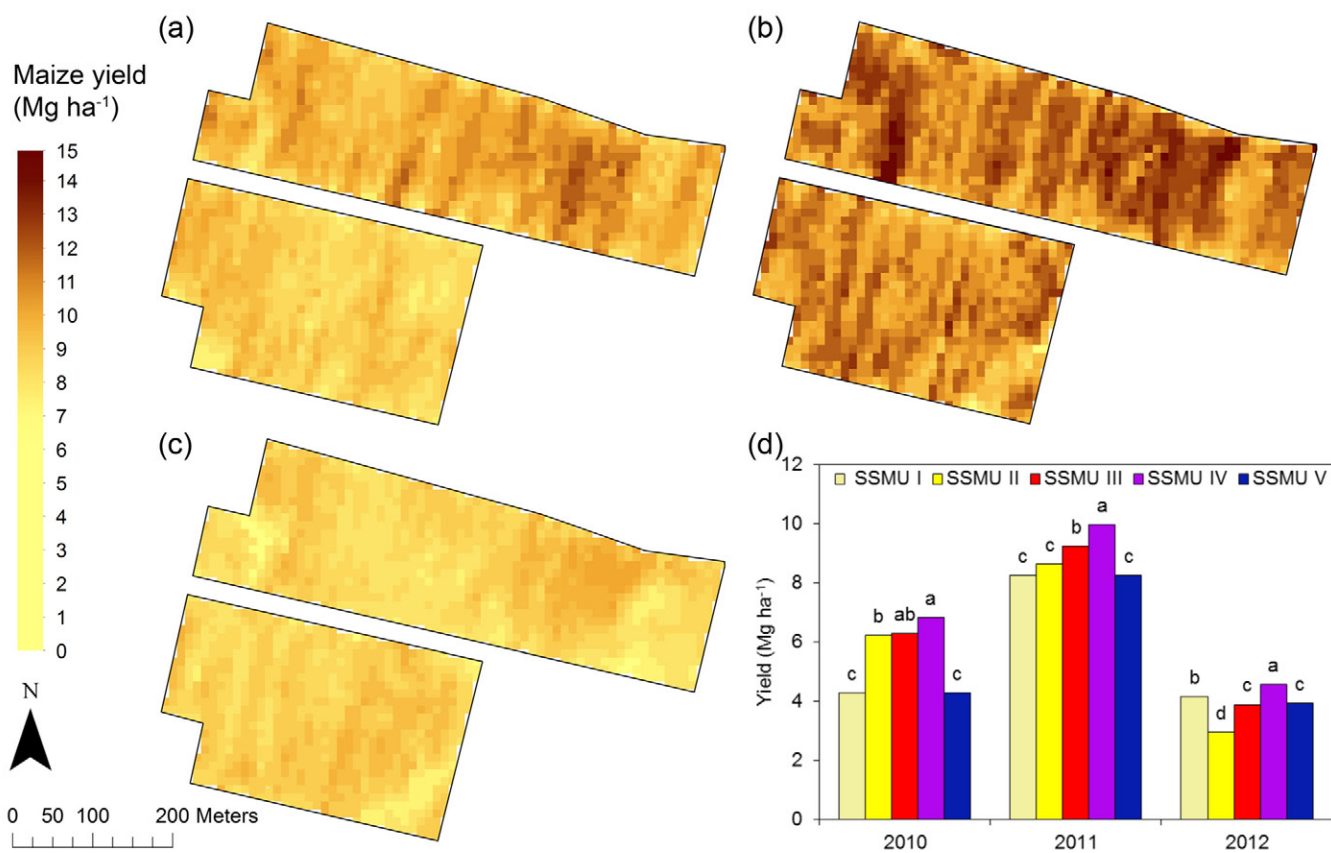


Fig. 3. Yield maps at the study site in (a) 2010, (b) 2011, and (c) 2012; and (d) average yield at each site-specific management unit (SSMU) through the 3 yr. Within years, SSMUs topped with the same letter are not significantly different ( $P < 0.05$ ).

### Yield Spatiotemporal Variability

The average maize yield (14% moisture) was  $6.0 \text{ Mg ha}^{-1}$ , with large differences among the 3 yr: 5.5, 8.8,  $3.9 \text{ Mg ha}^{-1}$  in 2010, 2011, and 2012, respectively. Unfortunately, maize production in 2010 was compromised by a heavy wind and hail storm ( $\sim 60 \text{ mm}$  of rainfall) occurring on 13 August (Scudiero et al., 2013). Hail and wind damaged many mature plants, making it impossible for the combine to harvest the ears. Due to the size of the study site, the storm hit the entire field uniformly. Therefore, yield spatial variability at the field scale was not believed to be too severely affected (Scudiero et al., 2013).

Spatial variance ( $4.6 \text{ Mg ha}^{-1}$ ) and temporal variance ( $9.2 \text{ Mg ha}^{-1}$ ) across the 3 yr suggested that climatic conditions governed the production variability even more than soil variability. This is usually expected, even in areas characterized by contrasting soils (McBratney et al., 2005).

The three yield maps shown in Fig. 3 clearly highlight a spatial pattern at the field scale. The most productive area in the 3 yr was SSMU IV, while, probably due to rainfall scarcity and low water holding capacity (Table 1), the sandy SSMU III was characterized by a yield significantly lower than SSMU IV in 2011 and 2012 (Fig. 3d). Salinity did not significantly affect maize yield in the rainy 2010, but affected maize yield much more in the following 2 yr, when the saline SSMU II was the least productive area. In 2011, SSMUs I and V were also characterized by the lowest yield values.

Yield data showed significant ( $p < 0.01$ ) linear correlations between 2010 and 2011, 2010 and 2012, and 2011 and 2012, with Pearson correlation coefficients ( $r$ ) of 0.50, 0.24, and 0.40, respectively. According to the cross-covariograms (Fig. 4),

positive spatial dependency among yield maps was also observed. The strength of the spatial correlations varied according to the Pearson correlation coefficients. The stronger correlation at 20 m (i.e., one lag distance) was clearly observed between 2010 and 2011, with a cross-covariance  $\sim 1.0$ . Smaller cross-covariance values were observed between 2011 and 2012 and between 2010 and 2012, at 0.75 and 0.38, respectively. The distance at which the cross-covariance was  $< 0.05$  was 125, 114, and 90 m for the year couples 2010 with 2011, 2011 with 2012, and 2010 with 2012, respectively.

As the spatial structure of production was considered fairly stable with time, a maize yield spatial trend map was created (Fig. 5a). The map confirmed that SSMU IV was characterized by the highest yield, with the production in the saline SSMU II lower than in the coarse-textured SSMU III but higher than in SSMUs I and V (Fig. 5b). Low temporal variability is supported by the significant correlations described above, although their low values imply that yield temporal variability through the growing seasons was considerable.

Figure 5c shows the yield temporal variability map for the study area. A clear pattern cannot be identified in Fig. 5. Nevertheless, the low-production and moderately saline SSMUs I and V were characterized by temporal variability significantly lower than the other three units (Fig. 5d).

### Normalized Difference Vegetation Index Variability Analysis

The CropCircle NDVI data sets were interpolated into 10-by-10-m grid maps (Fig. 6) giving low cross-validation errors (Table 3). In all 3 yr, NDVI decreased from Surveys i to iii,

Table 3. Normalized difference vegetation index (NDVI) data summary statistics: mean and range, exponential isotropic semivariogram specifications, and cross-validation root mean square error (RMSE).

Year	Date	NDVI survey	Avg.	Min.	Max.	SD	Exponential isotropic semivariogram specifications				Cross-validation RMSE
							Nugget	Partial sill	Lag	Range	
2010	9 July	i	0.696	0.503	0.750	0.024	0.0001	0.0002	20	47.1	0.02
	23 July	ii	0.638	0.485	0.718	0.044	0.0001	0.0003	25	195.3	0.02
	16 Aug.	iii	0.576	0.357	0.694	0.051	0.0001	0.0003	20	114.6	0.03
2011	4 July	i	0.702	0.593	0.743	0.022	0.0001	0.0001	20	68.6	0.02
	14 July	ii	0.680	0.561	0.750	0.026	0.0001	0.0002	20	77.3	0.02
	5 Aug.	iii	0.568	0.349	0.827	0.087	0.0001	0.0006	20	158.0	0.04
2012	15 June	i	0.734	0.576	0.829	0.038	0.0004	0.0003	20	164.6	0.04
	27 June	ii	0.703	0.572	0.771	0.035	0.0000	0.0003	20	84.0	0.02
	19 July	iii	0.583	0.419	0.713	0.065	0.0000	0.0005	20	148.0	0.02

Table 4. Pearson correlations between yield maps in 2010, 2011, and 2012 and the normalized difference vegetation index (NDVI) provided by each survey (i, ii, and iii) and the intra-annual NDVI spatial trend (NDVI\_SpT) and temporal variability (SDVI). All correlations are significant at the  $p < 0.05$  level.

Yield map	Pearson correlation				
	i	ii	iii	NDVI_SpT	SDVI
2010	0.21	0.58	0.41	0.57	0.21
2011	0.43	0.26	0.48	0.51	0.46
2012	0.48	0.39	0.69	0.68	0.60

as typically observed in maize during the reproduction phase (Cairns et al., 2012; Raun et al., 2005; Solari et al., 2008). The spatial variability of NDVI maps generally increased during each growing season, indicating that stresses occurring during R1 and R2 can strongly limit production (Abendroth et al., 2011; NeSmith and Ritchie, 1992). The NDVI spatial variances for Surveys i, ii, and iii were  $0.6 \times 10^{-3}$ ,  $1.9 \times 10^{-3}$ , and  $2.5 \times 10^{-3}$ , respectively, in 2010;  $0.5 \times 10^{-3}$ ,  $6.7 \times 10^{-3}$ , and  $7.5 \times 10^{-3}$ , respectively, in 2011; and  $1.4 \times 10^{-3}$ ,  $1.1 \times 10^{-3}$ , and  $4.5 \times 10^{-3}$ , respectively, in 2012.

All NDVI maps were significantly correlated ( $p < 0.05$ ) with the relative yield map (Table 4), showing that they could be used to represent maize yield. Indeed, Weber et al. (2012) concluded that anthesis (right before R1) and R2 are the stages when maize reflectance best reflects maize grain yield. The stronger relationships between NDVI and the yield maps were observed in Surveys ii, iii, and iii for the 2010, 2011, and 2012 growing seasons, respectively; in these three cases, the cross-covariance at 20 m and the distance where it was  $< 0.05$  were 0.58, 0.44, and 0.56 and 180 m, 151 m, 98 m, respectively. Spatial correlations between NDVI and yield in 2010 were of the same magnitude as those related to 2011 and 2012, confirming that the spatial pattern of maize production was not affected too severely by the wind and hail storm that occurred on 13 Aug. 2010. The NDVI also showed significant correlations with plant height, aerial biomass, and leaf osmotic potential measured at some selected locations in the study area in 2010 and 2011 (Scudiero et al., 2011, 2014).

### Interannual Normalized Difference Vegetation Index Variability

The NDVI interannual spatial trend map (Fig. 7a) was strongly ( $p < 0.05$ ) correlated with the yield spatial trend map (Table 5). The correlation was characterized by an  $r$  value

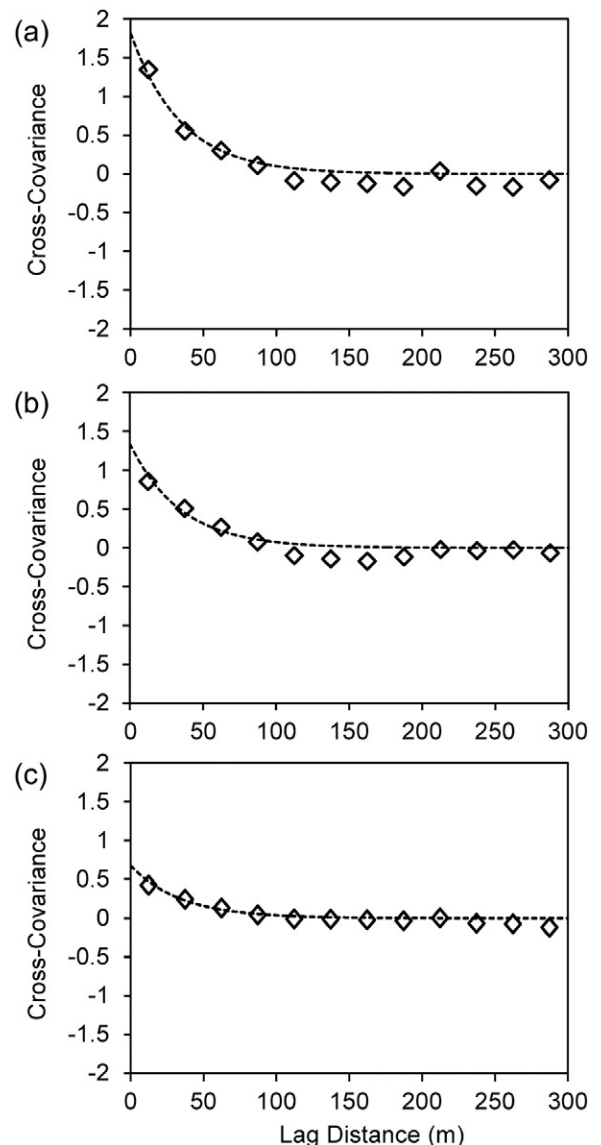


Fig. 4. Experimental (squares) and fitted (dashed line) cross-covariograms between yield data in (a) 2010 and 2011, (b) 2011 and 2012, and (c) 2010 and 2012.

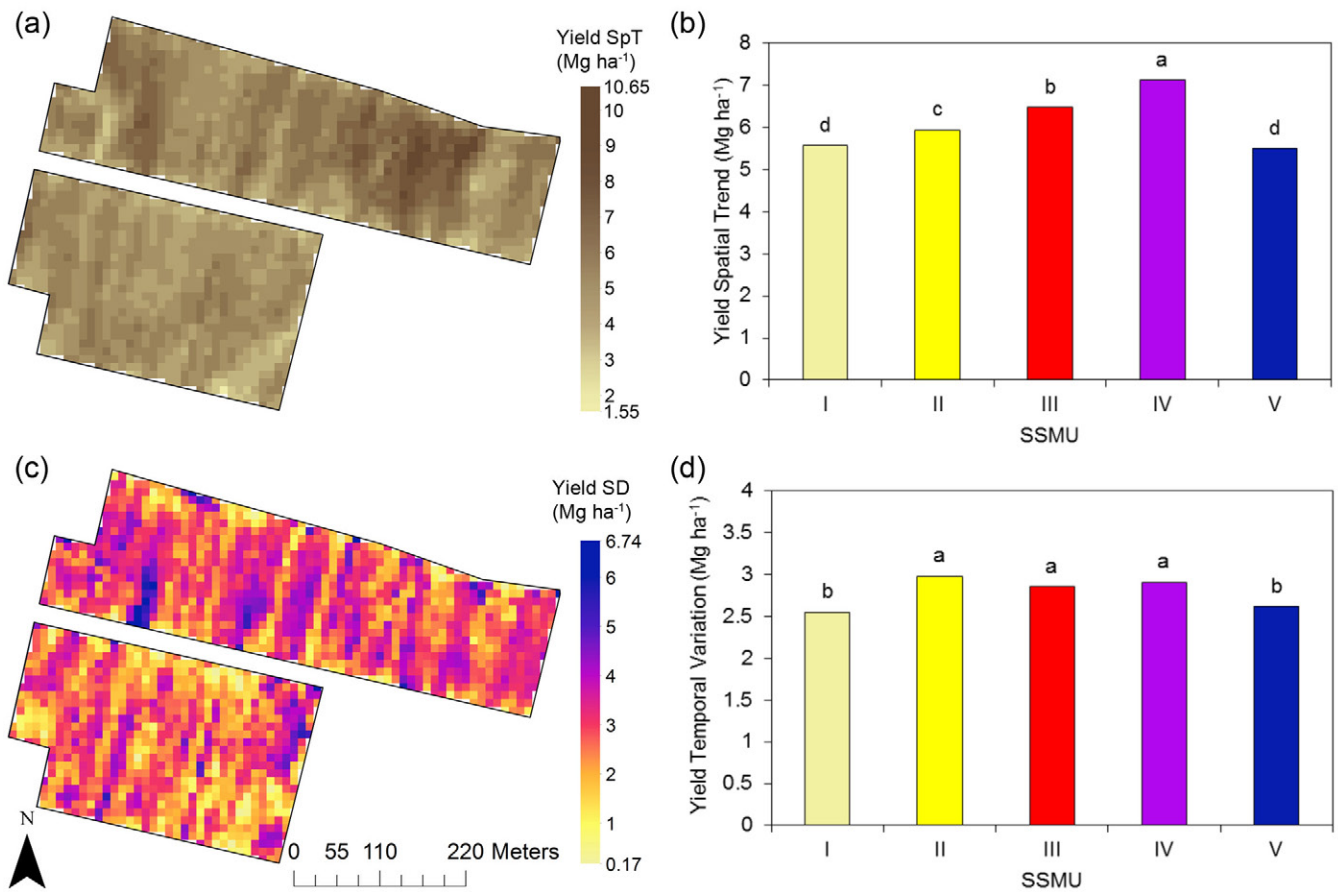


Fig. 5. (a) Yield map and (b) comparison within soil-specific management units (SSMUs) of maize yield spatial trend (SpT); and (c) variability map and (d) comparison within SSMUs of maize yield temporal variation (SD). Columns topped with the same letter are not significantly different ( $P < 0.05$ ).

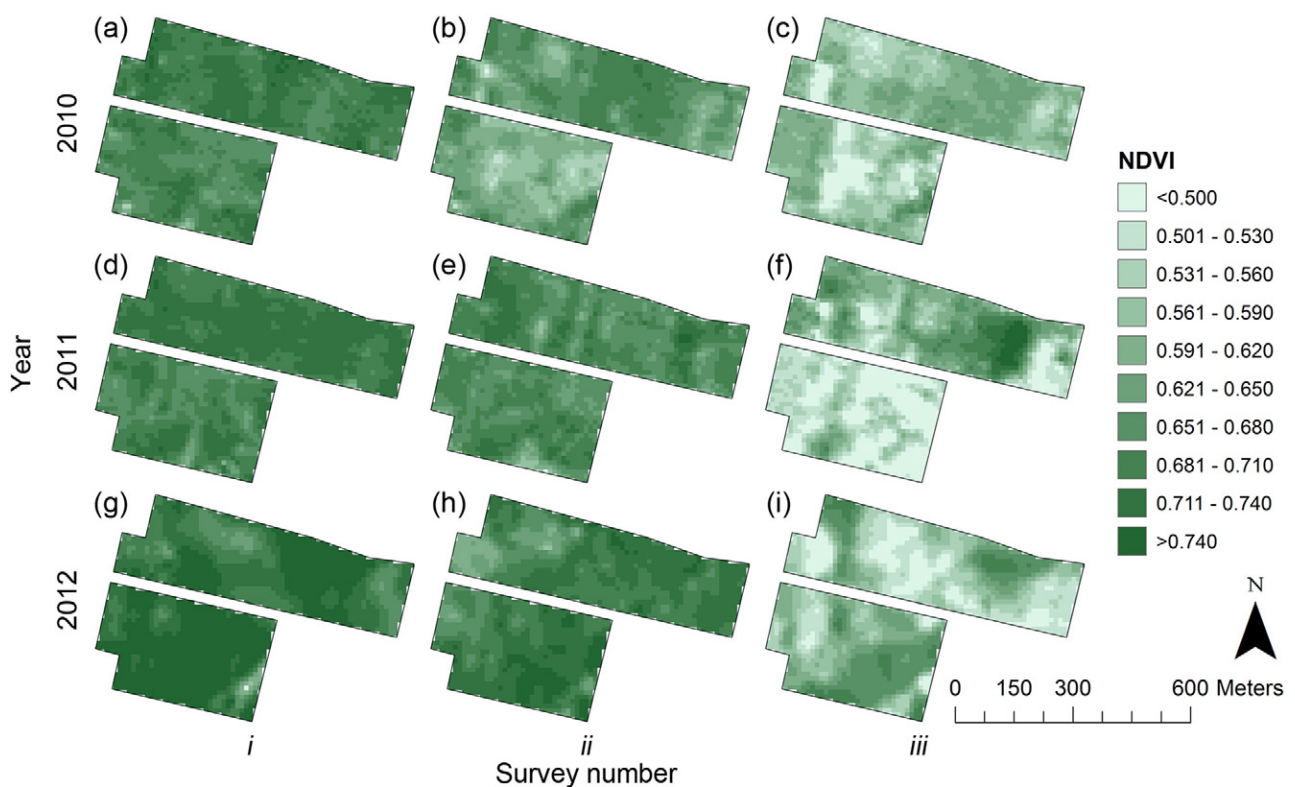


Fig. 6. Normalized difference vegetation index (NDVI) maps from (a) 9 July 2010, (b) 23 July 2010, (c) 16 Aug. 2010, (d) 4 July 2011, (e) 14 July 2011, (f) 5 Aug. 2011, (g) 15 June 2012, (h) 27 June 2012, and (i) 19 July 2012.

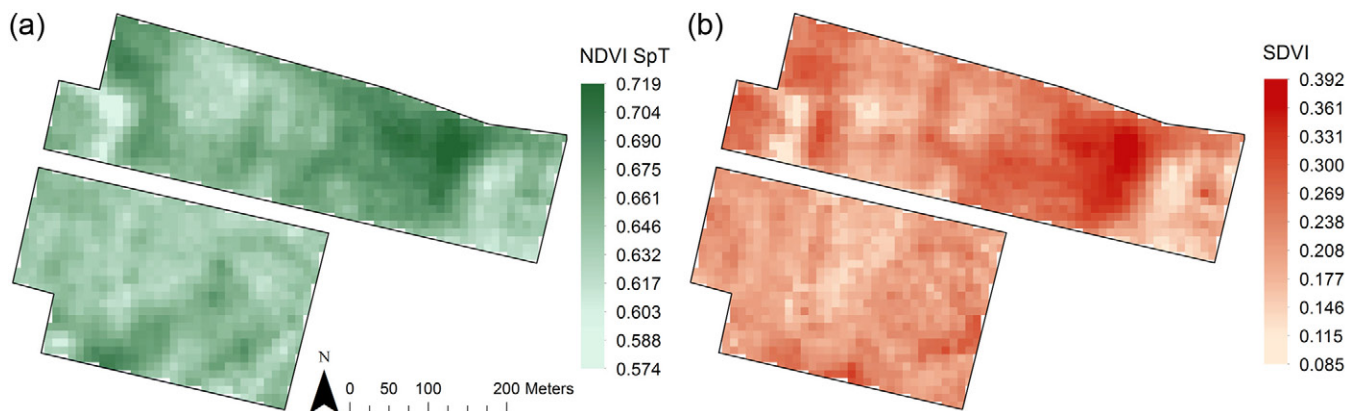


Fig. 7. Interannual normalized difference vegetation index (a) spatial trend (NDVI SpT) and (b) temporal variability (SDVI).

higher than most of the correlation coefficients between the single NDVI surveys and the corresponding yield maps. The interannual NDVI spatial trend was also significantly correlated ( $r = 0.23, p < 0.05$ ) with the root-zone clay fraction measured at the soil sampling locations (data not shown). Indeed, as highlighted by Scudiero et al. (2013) at the study site, high yield was associated with high clay contents. On the other hand, the NDVI spatial trend did not show significant correlations with soil salinity, organic C content, or bulk density, which, together with clay content, are responsible for the yield spatial variability at the study site (Scudiero et al., 2013).

The interannual SDVI map (Fig. 7b) was positively correlated ( $p < 0.05$ ) with the yield spatial trend map (Table 5), indicating that the lower the NDVI temporal variability is through the years, the lower the yield. Maps of NDVI\_SpT and SDVI were characterized by different relationships between the SSMUs (Table 6). The interannual NDVI spatial trend was significantly different among all SSMUs. The highest NDVI was for SSMU IV, followed by SSMUs III, I, II, and V, similarly to what was observed for the yield spatial trend map (Fig. 5b). On the other hand, the significant differences in SDVI values between SSMUs (Table 6) confirmed that the effects of saline stress on crop-canopy reflectance are more stable with time than other types of stress. Indeed, the saline SSMU II and the moderately saline SSMUs I and V showed much lower SDVI values than SSMUs III and IV. On the other hand, SSMU III was not significantly different from SSMU IV in terms of SDVI, which is contrary to what was observed for the spatial trend maps of NDVI (Table 6) and yield (Fig. 5b). Moreover, SDVI and root-zone soil salinity were significantly correlated ( $r = -0.33, p < 0.01$ ) at the sampling locations, while no significant correlation was observed between SDVI and clay content, soil organic C, or bulk density.

The low temporal variability of crop reflectance in saline soils was already highlighted for salinity values higher (Furby et al., 2010; Madrigal et al., 2003) and at spatial resolution larger (Furby et al., 2010; Lobell et al., 2010; Madrigal et al., 2003) than those characterizing this study. Indeed, the results presented show that the relationship is also significant when ground-based NDVI measurements at a fairly high spatial resolution ( $100 \text{ m}^2$ ) are used over a field characterized by high spatial heterogeneity of soil properties and moderate to fairly high salinity values (Fig. 2b; maximum  $EC_{1:2} = 3.3 \text{ dS m}^{-1} \approx EC_e = 19.8 \text{ dS m}^{-1}$ ). However, it was not possible to build a regression-based spatial model relating low temporal canopy

reflectance variability to soil salinity, as suggested by Lobell et al. (2010), because the resulting salinity estimations were characterized by large errors. Lobell et al. (2010) used 6 yr of reflectance data in a large area ( $17000 \text{ km}^2$ ) where salinity was likely to be the main reason for crop stress. In this study, the effects of other stress types on crop status are remarkable (Scudiero et al., 2013). Possibly, 3 yr of data might have not been enough to quantify the effects of soil salinity alone on crop growth.

#### Intra-annual Normalized Difference Vegetation Index Variability

The intra-annual NDVI spatial trend maps (not shown) generally exhibited higher  $r$  values with their respective yield maps than the single NDVI surveys did (Table 4). Again, the intra-annual SDVI maps (Fig. 8) showed that zones with low annual NDVI temporal variation were generally characterized by low maize yield (Table 4). Nevertheless, these NDVI temporal variability relationships with yield were characterized by low  $r$  values, indicating that most of the intra-annual NDVI temporal variability was not linked to yield spatiotemporal variability.

The intra-annual SDVI varied greatly within the five SSMUs (Fig. 8d). The SDVI map in 2011 was characterized by the highest values, recorded in SSMU IV. The lowest SDVI values were observed in SSMU II as in 2012. In general, the SSMUs I, II,

Table 5. Pearson correlations between maps of yield spatial trend and temporal variability with interannual NDVI spatial trend and temporal variability. All correlations are significant at the  $p < 0.05$  level.

Yield map	Pearson correlation	
	Spatial trend	Temporal variability
Spatial trend	0.67	0.59
Temporal variability	0.10	0.11

Table 6. Mean values of the normalized difference vegetation index spatial trend (NDVI\_SpT) and temporal variability (SDVI) for the five soil-specific management units (SSMUs).

SSMU	NDVI_SpT	SDVI
I	0.651 c†	0.215 b
II	0.646 d	0.200 c
III	0.659 b	0.248 a
IV	0.671 a	0.248 a
V	0.641 e	0.197 c

† Means followed by different letters are significantly different between SSMUs at the  $p < 0.05$  level according to the Kruskal–Wallis test

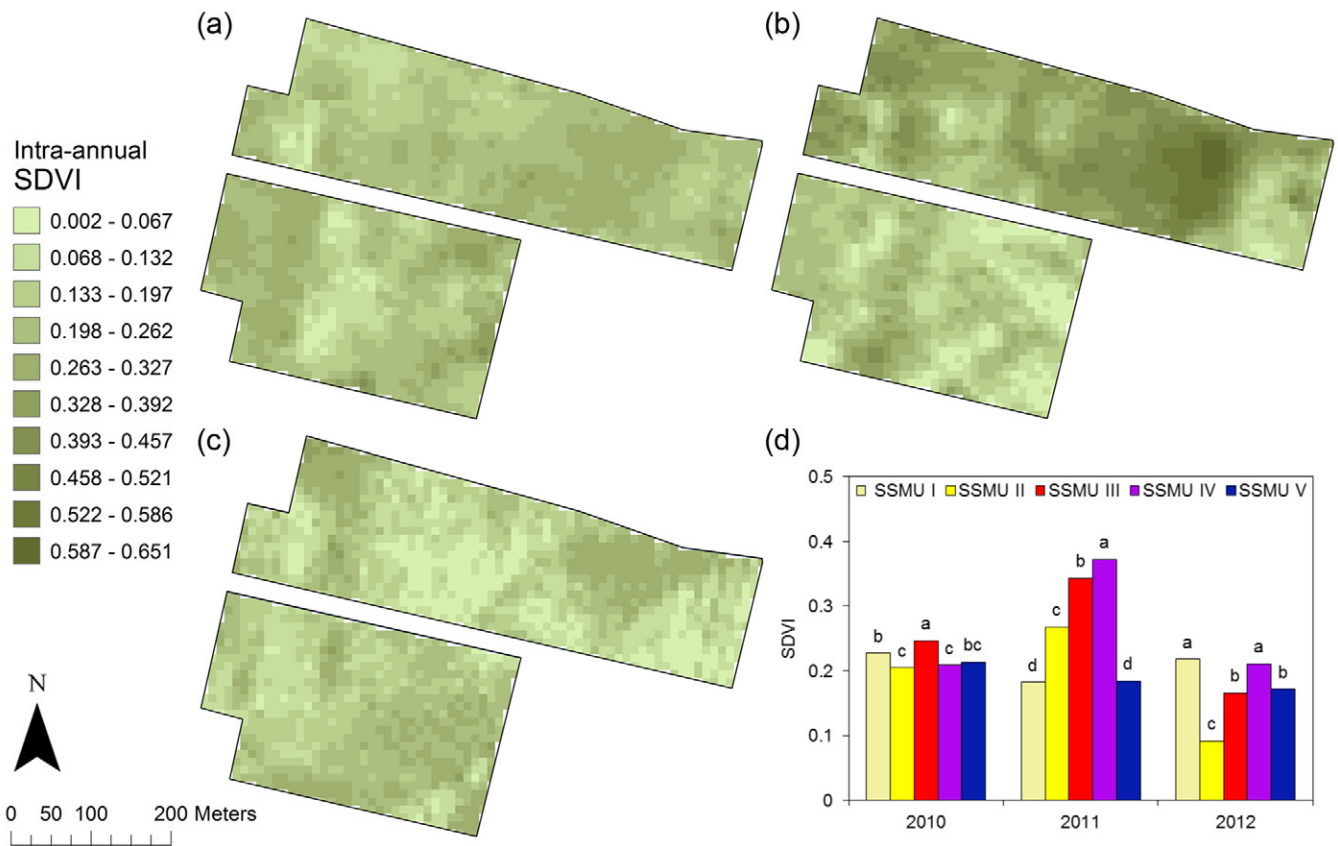


Fig. 8. Intra-annual temporal variability of the normalized difference vegetation index (SDVI) in (a) 2010, (b) 2011, and (c) 2012; and (d) average SDVI at each site-specific management unit (SSMU) through the 3 yr. Within years, SSMUs topped with the same letter are not significantly different ( $P < 0.05$ ).

and V were characterized by low SDVI values during the 3 yr. In the rainy 2010, SSMU III (low clay and high bulk density) was characterized by the highest SDVI values. In the following drier years, SSMU III came second to SSMU IV in terms of SDVI values. In particular, in 2012, the SDVI in SSMU III was not significantly different than that in SSMU V, yet still higher than that in SSMU II. The intra-annual SDVI was only significantly correlated with root-zone salinity in 2010 ( $r = -0.31, p < 0.01$ ). On the other hand, it was significantly correlated with clay content only in 2010 ( $r = -0.36, p < 0.01$ ) and 2011 ( $r = 0.27, p < 0.01$ ). No significant correlations were observed between soil organic C or bulk density and intra-annual SDVI.

At the five monitoring stations, the evapotranspiration reduction coefficient  $K_s$  (Eq. [6]) quantified water and/or salinity stresses during the three growing seasons. Plants were affected by soil salinity stress at Stations A, C, and D, where the salinity was above the  $EC_{e\_threshold} = 1.7 \text{ dS m}^{-1}$  (Table 1). Because Station C was characterized by a very shallow water table during the 3 yr ( $\sim 50\text{--}60 \text{ cm}$ ), the daily  $K_s$  ( $= 0.64$ ) was influenced only by salt stress. In 2011 and 2012, both salinity and water stress affected crop development at Stations A and D. Stations B and E were not affected by salt stress because the  $EC_e$  was much smaller than the  $EC_{e\_threshold}$  (Table 1). However, severe water stress was experienced at these stations, particularly in 2011 and 2012, because they were both located on paleochannels in SSMU III with a sand percentage of  $\sim 70\%$ . The daily  $K_s$  estimates at Stations B and E were strongly correlated, with  $r = 0.99$  in 2011 and  $r = 0.86$  in 2012, whereas no significant correlations were observed between the  $K_s$  values of the other stations, indicating

that the SSMU delineation properly identified fairly homogeneous soil clusters that were noticeably different between each other.

The relationship between the NDVI change through surveys ( $\Delta\text{NDVI}$ ) and  $K_s$  can help describe and understand the influence of the two stress types on crop development (Fig. 9). The data from Stations B and E relative to the last NDVI surveys of 2011 and 2012 were removed from the relationship because they showed a very large NDVI drop, typically observed in maize plants undergoing early canopy senescence due to strong stress events (Cairns et al., 2012; Raun et al., 2005; Wolfe et al., 1988). At these stations, the NDVI drop was caused by excessive water stress, with water contents very close to the wilting point. As a matter of fact, water stress around Station E was so extreme in 2012 that all plants died before ear formation (yield =  $0 \text{ Mg ha}^{-1}$ ).

About 44% ( $p < 0.05$ ) of the NDVI change at the monitoring stations could be explained by  $\Sigma K_s$  (Fig. 9), indicating that: (i) both saline and water stresses were of great influence on canopy reflectance at the study site; and (ii) in the reproductive phase before full maturity, the higher soil the salinity and/or water stress, the lower the (intra-annual) NDVI temporal variation. As suggested by Fig. 8, the efforts of mapping salinity using reflectance measurements from a single year encounter a great risk of producing poor results (Lobell et al., 2010): the intra-annual analysis does not allow emphasizing the soil features that are more stable with time, as multiyear analysis does (Lobell et al., 2010). Intra-annual analysis could be useful, on the other hand, to identify the areas of a field that are more affected by the factors limiting crop yield during a single growing season. This could potentially allow farmers

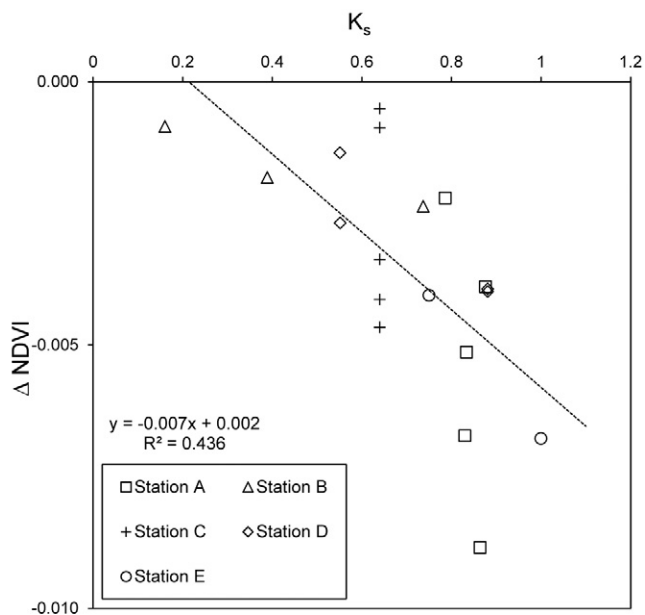


Fig. 9. Intra-annual relationship between the daily average variations of the normalized difference vegetation index ( $\Delta$ NDVI) and the evapotranspiration reduction coefficient  $K_s$  between consecutive NDVI surveys at the five soil monitoring stations.

to plan site-specific management if similar conditions (e.g., meteorological) arise in following years.

It is worth noting that the relation showed in Fig. 9 described only plants under stress, and a non-stressed control is missing. Moreover, the collected data are suitable to describe only the NDVI decrease typically observed in the reproduction physiological phase of maize (Cairns et al., 2012; Raun et al., 2005). It would also be of great interest to understand how the NDVI increase typical of the vegetative phase of maize could be influenced by water stress and/or salinity. In addition, the study of reflectance throughout the whole growing season would help reduce possible biasing effects of NDVI saturation typically observed in the late V and early R stages, especially in very healthy vegetation (Cairns et al., 2012; Gitelson, 2004; Raun et al., 2005). Indeed, saturated NDVI signals in healthy plants would lower the temporal variability of the NDVI, consequently weakening the relationship of the latter with soil salinity.

## SUMMARY AND CONCLUSIONS

Spatiotemporal variability of maize yield is greatly affected by the spatial variability of soil properties (i.e., soil salinity) and temporal changes in meteorological conditions (i.e., water availability). These relationships were investigated in a field at the Venice Lagoon margin where crop production, canopy reflectance, and soil quality were monitored between 2010 and 2012. The major challenge of this work was to discriminate the effects of saline and water stresses on the yield spatiotemporal variability using multiple surveys of ground-based crop reflectance acquired during the reproductive phase of maize.

The results confirm that the use of NDVI maps is a viable means of describing crop growth and production variability. In particular, the following specific outcomes were found:

- The analysis of intra-annual (i.e., within a single year) NDVI spatiotemporal variability provides a means of understanding stress onset and impact on a crop according to soil variability and meteorological conditions. The combined action

of the two stresses was responsible for much of the NDVI reduction ( $\sim 44\%$ ) with time at some selected locations of the study field. However, the intra-annual analysis does not allow distinguishing between the two stress types.

- The interannual (i.e., across the 3 yr) NDVI spatiotemporal variability can identify areas where stress is fairly stable through the years and areas where soil-water content enhances or mitigates soil-plant interactions. The NDVI interannual temporal variability in saline areas was significantly lower than in zones of optimal maize growth affected by water stress only. However, where the two stresses superposed, the interannual NDVI temporal variability was so small (even at low salinity values) that the distinction between the areas affected only by salinity and those affected also by water stress is unachievable.
- The low temporal variability of plant reflectance over saline soils was previously observed by others (Furby et al., 2010; Lobell et al., 2010; Madrigal et al., 2003) at large spatial resolutions ( $>900 \text{ m}^2$ ) and with salinity values generally higher than those observed at the Venice Lagoon margin ( $EC_e < 20 \text{ dS m}^{-1}$ ). Contrary to most satellite sensors, ground-based NDVI acquisitions allow measuring crop reflectance at fairly high spatial resolution ( $\sim 100 \text{ m}^2$ ). The results show that interannual NDVI variability can be effectively used to assess soil salinity even over highly heterogeneous areas.

In conclusion, studying multiple-year crop reflectance data allows refining agronomical practices, especially in areas characterized by high soil spatial variability and the insurgence of various types of edaphic stress. In fact, the larger the number of growing seasons considered, the stronger the relationships between crop reflectance and soil properties become. Because soil salinity is a common issue around the world, studying canopy reflectance across multiple years can be very beneficial for precision agriculture practices (e.g., precision irrigation), particularly in environments where water availability is scarce or irrigation water quality is poor. Future research should focus on analyses of spatiotemporal soil-plant interactions at a regional scale by using high-resolution reflectance images provided by the latest generation of satellite sensors.

## ACKNOWLEDGMENTS

This study was funded within the Research Program “GEO-RISKS: Geological, Morphological and Hydrological Processes: Monitoring, Modeling and Impact in the North-Eastern Italy: Work package 4”, the University of Padua, Italy. We acknowledge the outstanding work of Davide Piragnolo and Diego Mengardo, who helped in the laboratory analyses and field surveys.

## REFERENCES

- Abendroth, L.J., R.W. Elmore, M.J. Boyer, and S.K. Marlay. 2011. Corn growth and development. PMR 1009. Iowa State Univ. Ext., Ames.
- Acevedo-Opazo, C., B. Tisseyre, S. Guillaume, and H. Ojeda. 2008. The potential of high spatial resolution information to define within-vineyard zones related to vine water status. *Precis. Agric.* 9:285–302. doi:10.1007/s11119-008-9073-1
- Allen, R.G., L.S. Pereira, D. Raes, and M. Smith. 1998. Crop evapotranspiration. Guidelines for computing crop water requirements. Irrig. Drain. Pap. 56. FAO, Rome.
- Blackmer, T., J. Schepers, and G. Meyer. 1995. Remote sensing to detect nitrogen deficiency in corn. In: P.C. Robert et al., editors, Site-specific management for agricultural systems. ASA, CSSA, and SSSA, Madison WI. p. 505–512.

- Blackmore, S. 1999. Remedial correction of yield map data. *Precis. Agric.* 1:53–66. doi:10.1023/A:1009969601387
- Blackmore, S. 2000. The interpretation of trends from multiple yield maps. *Comput. Electron. Agric.* 26:37–51. doi:10.1016/S0168-1699(99)00075-7
- Blackmore, S., R.J. Godwin, and S. Fountas. 2003. The analysis of spatial and temporal trends in yield map data over six years. *Biosyst. Eng.* 84:455–466. doi:10.1016/S1537-5110(03)00038-2
- Box, G.E.P., and D.R. Cox. 1964. An analysis of transformations. *J.R. Stat. Soc., Ser. B* 26:211–252.
- Cairns, J.E., C. Sanchez, M. Vargas, R. Ordoñez, and J.L. Araus. 2012. Dissecting maize productivity: Ideotypes associated with grain yield under drought stress and well-watered conditions. *J. Integr. Plant Biol.* 54:1007–1020. doi:10.1111/j.1744-7909.2012.01156.x
- Corwin, D.L., S.M. Lesch, P.J. Shouse, R. Soppe, and J.E. Ayars. 2003. Identifying soil properties that influence cotton yield using soil sampling directed by apparent soil electrical conductivity. *Agron. J.* 95:352–364. doi:10.2134/agronj2003.0352
- de Franco, R., G. Biella, L. Tosi, P. Teatini, A. Lozej, B. Chiozzotto, et al. 2009. Monitoring the saltwater intrusion by time lapse electrical resistivity tomography: The Chioggia test site (Venice Lagoon, Italy). *J. Appl. Geophys.* 69:117–130. doi:10.1016/j.jappgeo.2009.08.004
- Dobermann, A., and J.L. Ping. 2004. Geostatistical integration of yield monitor data and remote sensing improves yield maps. *Agron. J.* 96:285–297. doi:10.2134/agronj2004.0285
- Elmetwalli, A.M.H., A.N. Tyler, P.D. Hunter, and C.A. Salt. 2012. Detecting and distinguishing moisture- and salinity-induced stress in wheat and maize through in situ spectroradiometry measurements. *Remote Sens. Lett.* 3:363–372. doi:10.1080/01431161.2011.599346
- FAO-UNESCO. 1989. Soil map of the world, revised legend. FAO, Rome.
- Furby, S., P. Caccetta, and J. Wallace. 2010. Salinity monitoring in Western Australia using remotely sensed and other spatial data. *J. Environ. Qual.* 39:16–25. doi:10.2134/jeq2009.0036
- Gitelson, A.A. 2004. Wide dynamic range vegetation index for remote quantification of biophysical characteristics of vegetation. *J. Plant Physiol.* 161:165–173. doi:10.1078/0176-1617-01176
- Goovaerts, P. 1997. Geostatistics for natural resources evaluation. Oxford Univ. Press, New York.
- Hu, Y., Z. Burucs, S. von Tucher, and U. Schmidhalter. 2007. Short-term effects of drought and salinity on mineral nutrient distribution along growing leaves of maize seedlings. *Environ. Exp. Bot.* 60:268–275. doi:10.1016/j.envexpbot.2006.11.003
- Kruskal, W.H., and W.A. Wallis. 1952. Use of ranks in one-criterion variance analysis. *J. Am. Stat. Assoc.* 47:583–621. doi:10.1080/01621459.1952.10483441
- Letey, J., and A. Dinar. 1986. Simulated crop-water production functions for several crops when irrigated with saline waters. *Hilgardia* 54:1–32.
- Lobell, D.B., S.M. Lesch, D.L. Corwin, M.G. Ulmer, K.A. Anderson, D.J. Potts, et al. 2010. Regional-scale assessment of soil salinity in the Red River Valley using multi-year MODIS EVI and NDVI. *J. Environ. Qual.* 39:35–41. doi:10.2134/jeq2009.0140
- Lobell, D.B., J.I. Ortiz-Monasterio, F.C. Gurrola, and L. Valenzuela. 2007. Identification of saline soils with multiyear remote sensing of crop yields. *Soil Sci. Soc. Am. J.* 71:777–783. doi:10.2136/sssaj2006.0306
- Maas, E. 1996. Crop salt tolerance. In: K.K. Tanji, editor, *Agricultural salinity assessment and management*. ASCE Manual 71. Am. Soc. Civ. Eng., New York. p. 262–304.
- Madrigal, L.P., C.L. Wiegand, J.G. Meraz, B.D.R. Rubio, X.C. Estrada, and O.L. Ramirez. 2003. Soil salinity and its effect on crop yield: A study using satellite imagery in three irrigation districts. *Ing. Hidraul. Mex.* 18:83–97.
- Manoli, G., E. Scudiero, M. Putti, F. Morari, and P. Teatini. 2014. Farmland productivity under stress conditions: A field scale monitoring and modeling study on the Venice coastland, Italy. Paper presented at: EGU General Assembly, Vienna. 27 Apr.–2 May 2014.
- Manoli, G., S. Bonetti, E. Scudiero, P. Teatini, P.J. Binning, F. Morari, et al. 2013. Monitoring and modeling farmland productivity along the Venice coastland, Italy. *Procedia Environ. Sci.* 19:361–368. doi:10.1016/j.proenv.2013.06.041
- McBratney, A., B. Whelan, T. Ancev, and J. Bouma. 2005. Future directions of precision agriculture. *Precis. Agric.* 6:7–23. doi:10.1007/s11119-005-0681-8
- Mulla, D.J. 2013. Twenty five years of remote sensing in precision agriculture: Key advances and remaining knowledge gaps. *Biosyst. Eng.* 114:358–371. doi:10.1016/j.biosystemseng.2012.08.009
- Munns, R. 2002. Comparative physiology of salt and water stress. *Plant Cell Environ.* 25:239–250. doi:10.1046/j.0016-8025.2001.00808.x
- NeSmith, D.S., and J.T. Ritchie. 1992. Effects of soil water-deficits during tassel emergence on development and yield component of maize (*Zea mays* L.). *Field Crops Res.* 28:251–256. doi:10.1016/0378-4290(92)90044-A
- Ping, J.L., and A. Dobermann. 2005. Processing of yield map data. *Precis. Agric.* 6:193–212. doi:10.1007/s11119-005-1035-2
- Raun, W.R., J.B. Solie, K.L. Martin, K.W. Freeman, M.L. Stone, G.V. Johnson, and R.W. Mullen. 2005. Growth stage, development, and spatial variability in corn evaluated using optical sensor readings. *J. Plant Nutr.* 28:173–182. doi:10.1081/PLN-200042277
- Rhoades, J.D., F. Chanduvi, and S.M. Lesch. 1999. Soil salinity assessment: Methods and interpretation of electrical conductivity measurements. FAO, Rome.
- Rouse, J.W., Jr., R.H. Haas, J.A. Schell, and D.W. Deering. 1974. Monitoring vegetation systems in the Great Plains with ERTS. In: S.C. Freden et al., editors, *Third Earth Resources Technology Satellite Symposium*, Washington, DC. 10–14 Dec. 1973. NASA SP-351. U.S. Gov. Print. Office, Washington, DC. p. 309–317.
- Scudiero, E., A. Berti, P. Teatini, and F. Morari. 2012. Simultaneous monitoring of soil water content and salinity with a low-cost capacitance-resistance probe. *Sensors* 12:17588–17607. doi:10.3390/s121217588
- Scudiero, E., F. Braga, P. Teatini, D. Piragnolo, A. Berti, and F. Morari. 2011. Saltwater contamination in the Venice Lagoon margin, Italy: 2. The influence on the soil productivity: First results. In: S. Keesstra and G. Mol, editors, *Soil science in a changing world: Wageningen Conference on Applied Soil Science*, Wageningen, the Netherlands. 18–22 Sept. 2011. Wageningen Agric. Univ., Wageningen, the Netherlands. p. 95.
- Scudiero, E., P. Teatini, F. Braga, and F. Morari. 2014. Saltwater contamination and soil productivity at the southern margin of the Venice Lagoon, Italy. *In* D. Suarez and A. Dinar, editors, *Salinity Forum 2014*, Riverside, CA. 16–18 June 2014. Univ. of California, Riverside. p. 294–295.
- Scudiero, E., P. Teatini, D.L. Corwin, R. Deiana, A. Berti, and F. Morari. 2013. Delineation of site-specific management units in a saline region at the Venice Lagoon margin, Italy, using soil reflectance and apparent electrical conductivity. *Comput. Electron. Agric.* 99:54–64. doi:10.1016/j.compag.2013.08.023
- Shanahan, J.F., J.S. Schepers, D.D. Francis, G.E. Varvel, W.W. Wilhelm, J.M. Tringe, et al. 2001. Use of remote-sensing imagery to estimate corn grain yield. *Agron. J.* 93:583–589. doi:10.2134/agronj2001.933583x
- Sharp, R., and W. Davies. 1985. Root growth and water uptake by maize plants in drying soil. *J. Exp. Bot.* 36:1441–1456. doi:10.1093/jxb/36.9.1441
- Solari, F. 2006. Developing a crop based strategy for on-the-go nitrogen management in irrigated cornfields. Univ. of Nebraska, Lincoln.
- Solari, F., J. Shanahan, R. Ferguson, J. Schepers, and A. Gitelson. 2008. Active sensor reflectance measurements of corn nitrogen status and yield potential. *Agron. J.* 100:571–579. doi:10.2134/agronj2007.0244
- Tweed, S.O., M. Leblanc, J.A. Webb, and M.W. Lubczynski. 2007. Remote sensing and GIS for mapping groundwater recharge and discharge areas in salinity prone catchments, southeastern Australia. *Hydrogeol. J.* 15:75–96. doi:10.1007/s10040-006-0129-x
- Vina, A., A.A. Gitelson, D.C. Rundquist, G. Keydan, B. Leavitt, and J. Schepers. 2004. Monitoring maize (*Zea mays* L.) phenology with remote sensing. *Agron. J.* 96:1139–1147. doi:10.2134/agronj2004.1139
- Weber, V., J. Araus, J. Cairns, C. Sanchez, A. Melchinger, and E. Orsini. 2012. Prediction of grain yield using reflectance spectra of canopy and leaves in maize plants grown under different water regimes. *Field Crops Res.* 128:82–90. doi:10.1016/j.fcr.2011.12.016
- Whelan, B., and A. McBratney. 2000. The “null hypothesis” of precision agriculture management. *Precis. Agric.* 2:265–279. doi:10.1023/A:1011838806489
- Wolfe, D., D. Henderson, T. Hsiao, and A. Alvino. 1988. Interactive water and nitrogen effects on senescence of maize: I. Leaf area duration, nitrogen distribution, and yield. *Agron. J.* 80:859–864. doi:10.2134/agronj1988.00021962008000060004x